Differences in replication kinetics and cell tropism between neurovirulent and non-neurovirulent EHV1 strains during the acute phase of infection in horses

Annick C. Gryspeerdt, A.P. Vandekerckhove, B. Garré, F. Barbé, G.R. van de Walle, H.J. Nauwynck

Title: Differences in replication kinetics and cell tropism between neurovirulent and non-neurovirulent EHV1 strains during the acute phase of infection in horses

Authors: Annick C. Gryspeerdt, A.P. Vandekerckhove, B. Garré, F. Barbé, G.R. Van de Walle, H.J. Nauwynck

PII: S0378-1135(09)00535-5
DOI: doi:10.1016/j.vetmic.2009.10.015
Reference: VETMIC 4643

To appear in: *VETMIC*

Received date: 10-7-2009
Revised date: 13-10-2009
Accepted date: 16-10-2009

Please cite this article as: Gryspeerdt, A.C., Vandekerckhove, A.P., Garré, B., Barbé, F., Van de Walle, G.R., Nauwynck, H.J., Differences in replication kinetics and cell tropism between neurovirulent and non-neurovirulent EHV1 strains during the acute phase of infection in horses, *Veterinary Microbiology* (2008), doi:10.1016/j.vetmic.2009.10.015

Differences in replication kinetics and cell tropism between neurovirulent and non-neurovirulent EHV1 strains during the acute phase of infection in horses

Annick C. Gryspeerdt, A.P. Vandekerckhove, B. Garré, F. Barbé, G.R. Van de Walle[*#] *and H.J. Nauwynck*[*]

Laboratory of Virology, Department of Virology, Parasitology and Immunology, Faculty of Veterinary Medicine, Ghent University, Salisburylaan 133, 9820 Merelbeke, Belgium

[*] shared senior authorship

Number of text pages: 30

Number of tables:1

Number of figures: 8

Shortened running title: *In vivo* differences of EHV1 strains replication

[#] Corresponding author: Van de Walle Gerlinde

Laboratory of Virology, Department of Virology, Parasitology and Immunology

Faculty of Veterinary Medicine, Ghent University

Salisburylaan 133, 9820 Merelbeke, Belgium

Phone: 00 32 9 264 73 75

Fax: 00 32 9 264 74 95

E-mail: gerlinde.vandewalle@ugent.be

Abstract

Equine herpesvirus 1 (EHV1) replicates in the respiratory tract of horses, after which infected leukocytes transport virus throughout the body, resulting in abortion or nervous system disorders. Two EHV1 strains circulate in the field: neurovirulent and non-neurovirulent. To investigate differences in replication in the upper respiratory tract (URT), an experimental inoculation study in ponies was performed with both strains. Two groups of six ponies, were inoculated intranasally with $10^{6.5}$ $TCID_{50}$ of either strain. Clinical signs, nasal shedding and viremia were evaluated. At early time points post inoculation (pi), one pony of each group was euthanized. Tissues were collected for titration and immunostainings. Number and size of EHV1-induced plaques were calculated, and individual EHV1-infected cells were quantified and characterized. Inoculation with either strain resulted in nasal shedding and replication in several tissues of the URT. Both strains replicated in a plaquewise manner in epithelium of the nasal mucosa, but replication in epithelium of the nasopharynx was largely limited to non-neurovirulent EHV1. Plaques were never able to cross the basement membrane, but individual infected cells were noticed in the connective tissue of all examined tissues for both strains. The total number of these cells however, was 3-7 times lower with non-neurovirulent EHV1 compared to neurovirulent EHV1. $CD172a^+$ cells and CD5+ lymphocytes were important target cells for both strains. Interestingly, in lymph nodes, B-lymphocytes were also important target cells for EHV1, irrespective of the strain. Viremia was detected very early pi and infected cells were mainly $CD172a^+$ for both strains. In summary, these results are valuable for understanding EHV1 pathogenesis at the port of entry, the URT.

Keywords: EHV1, pathogenesis, strain differences, carrier cells

Introduction

Infectious respiratory tract disease has been recognized as the cause of major health problems in horses. The most important respiratory pathogen is equine herpesvirus 1 (EHV1) and infections with this virus cause serious economic losses in the horse industry worldwide (Allen and Bryans, 1986; Ostlund, 1993; van Maanen, 2002). The upper respiratory tract is the first line of defence against respiratory pathogens and is also the primary replication site of EHV1, where it causes upper respiratory disorders (Kydd et al., 1994a, b). In addition, EHV1 can spread via infected blood leukocytes to internal organs, for example the pregnant uterus, causing symptoms such as abortion and neonatal foal death (Allen and Bryans, 1986). EHV1 can also reach the central nervous system, where replication in endothelial cells results in severe nervous system disorders with frequent fatal outcome. Neurological disease in horses caused by infection with certain isolates of EHV1 is a severe condition which is poorly understood (McCartan et al., 1995; Stierstorfer et al., 2002; van der Meulen et al., 2003a). The pathogenesis for developing this devastating condition is largely unknown and full protection against these secondary and severe symptoms can not be obtained by vaccination with the currently available vaccines (Heldens et al., 2001; Goodman et al., 2006; van der Meulen et al., 2007). Therefore, an improvement of the existing vaccines and/or the development of alternative strategies for the prevention and treatment of EHV1-induced infections are necessary. Importantly, this implies a firm notice about the pathogenesis of EHV1 during the acute phase of infection.

It has been suggested that distinct isolates of EHV1, differing in pathogenic capacity, circulate in the field. Nugent et al. (2006) indicated that a single nucleotide polymorphism (SNP) in the DNA polymerase is strongly associated with neurological versus non-neurological disease outbreaks. Studies in naturally infected horses with nervous system disorders have revealed a more robust cell-associated viremia in horses infected with

neurovirulent isolates of EHV1, in contrast to horses infected with non-neurovirulent isolates (Allen and Breathnach, 2006). This was further confirmed by reverse genetic experiments of EHV1 strains with a sole mutation of the DNA polymerase SNP, where experimental inoculation with such strains altered neurologic disease in horses (Goodman et al., 2007; Van de Walle et al., 2009). Moreover, *in vitro* experiments with these strains revealed differences in leukocyte tropism which could explain the difference in clinical outcome (Goodman et al., 2007). Still, the exact identity of carrier cells susceptible to EHV1 infection and hereby responsible for dissemination of infectious virus to sites of secondary replication, is a matter of debate. Blood samples from experimentally infected ponies were collected and examined for the presence of neurovirulent EHV1 (Scott et al., 1983). Hereby, T-lymphocytes were found to be the most important cell fraction to harbor virus *in vivo*. However, no full characterization of these cells was performed. Different studies with *in vitro* EHV1-infected leukocytes have also been performed to determine the identity of these cells. Hereby, mainly monocytes were susceptible to infection with non-neurovirulent EHV1 (van der Meulen et al., 2000). After stimulation with mitogens, T-lymphocytes became more susceptible, followed by B-lymphocytes (van der Meulen et al., 2001). Despite these studies, information on possible differences between neurovirulent and non-neurovirulent EHV1 strains at the port of entry, and identity of carrier cells during viremia remains limited.

To investigate this, six Shetland ponies were experimentally inoculated with a neurovirulent EHV1 strain and six with a non-neurovirulent EHV1 strain. These animals were subsequently euthanized to collect different tissues of the upper respiratory tract. Tissues that were positive for EHV1 on titration were stained with markers for different cell types to determine and quantify the carrier cells of EHV1 in the upper respiratory tract. In addition, peripheral blood mononuclear cells (PBMC) were also collected to quantify and identify the infected cell type during cell-associated viremia.

Materials and methods

Horses

Twelve male Shetland ponies, between the age of 6 months and 2 years, were used in this study. They were housed inside isolated stables. They were fed daily with a commercial, complete feed. Drinking water and hay were supplied *ad libitum*.

Prior to the experiment, ponies were monitored for 4 weeks. Rectal temperatures were measured daily and complement-dependent seroneutralization (SN)-tests and immunoperoxidase monolayer assays (IPMA) were performed weekly to determine EHV-specific antibody titers.

Virus and inoculation

Ponies were divided into two groups of 6. For the first group the Belgian EHV1 strain 03P37, isolated from the blood of a paralytic horse in 2003, was used for inoculation (Garre et al., 2009; van der Meulen et al., 2003a). The second group was inoculated with the Belgian strain 97P70, which was isolated from an aborted fetus (van der Meulen et al., 2006). The strains were typed in the DNA polymerase as D_{752} and N_{752} respectively in cooperation with the Animal Health Trust in the United Kingdom (Nugent et al., 2006). Based on their origin and genotyping, these strains will be referred as neurovirulent and non-neurovirulent in this paper. Virus stocks used for inoculation were at the 6^{th} passage; 2 passages in rabbit kidney cells (RK13) and 4 subsequent passages in equine embryonic lung cells (EEL). Both viruses had virtually identical single-step growth properties in RK13 cells for intra- and extracellular virus yields at all tested time points post infection (data not shown).

Ponies were inoculated oronasally with 20 ml of a virus suspension containing $10^{6.5}$ tissue culture infectious dose $_{50}$ ($TCID_{50}$). Ten ml of the virus suspension was administered intranasally (5 ml per nostril) using a thin probe and 10 ml was inoculated orally with a syringe. The virus titer was confirmed by titration of the inoculum.

Serological examination

For the seroneutralization (SN)-test, two-fold dilution series of the sera were prepared in MEM. Fifty micro liter of these serial dilutions were incubated for 23 hours (h) at 37°C with a fixed number of infectious virus (300 $TCID_{50}$ of EHV1 strain Arabica in 50 µl). Hereafter, 25 µl of guinea pig complement was added. After 1 h of incubation, the mixture of serum, virus and complement was added to RK13 cells. Inoculated cultures were further incubated at 37°C in an atmosphere containing 5% CO_2. After 7 days of incubation, the cultures were analysed for the presence of cytopathic effect. The neutralization titer was calculated as the reciprocal of the highest dilution of the serum that was able to completely block EHV1 infection in RK13 cells.

For the immunoperoxidase monolayer assay (IPMA), RK13 cells were inoculated with 10^3 $TCID_{50}$ of the EHV1 strain 97P70. After 28 h, cells were washed, dried at 37°C for 1 h and stored at -20°C until use. Plates were thawed and subsequently fixed with 4% paraformaldehyde and a solution containing 1% hydrogen peroxide in methanol. Following extensive washing, serial 2-fold dilutions of the sera were added and cells were incubated for 1 h at 37°C. Cells were incubated with peroxidase-labeled goat anti-horse antibodies (Jackson ImmunoResearch Laboratories Inc., PA, USA) and after 1 h, a substrate solution of 3-amino-9-ethylcarbazole in 0.05 M acetate buffer with 0.05% hydrogen was added to each well. Following 20 minutes of incubation at 37°C, substrate solution was replaced with acetate buffer to block the enzymatic staining reaction. The IPMA titer was calculated as the

148 reciprocal value of the highest serum dilution that induced visual staining of infected RK13
149 cells as determined by light microscopy.
150
151 *Clinical examination*
152 Horses were monitored daily for clinical signs by physical examination and
153 measurement of rectal temperatures. Fever was defined as a rectal temperature ≥ 38.5°C.
154 During clinical examination, nasal discharge (serous, mucous or purulent), lymph node
155 swelling, tachypnea and coughing were evaluated. In addition, neurological exams were
156 performed.
157
158 *Virological examination*
159 Nasopharyngeal mucus samples were taken daily until euthanasia. Immediately after
160 collection, swabs were immersed in transport medium containing phosphate-buffered saline
161 (PBS) supplemented with 10% fetal calf serum (FCS), 1000 U/ml penicillin, 1 mg/ml
162 streptomycin and 0.5 mg/ml kanamycin. EHV1 in nasopharyngeal secretions was titrated on
163 monolayers of RK13 cells, exactly as described previously (van der Meulen et al., 2003b).
164 On 1, 2, 3, 4, 5 and 7 days post inoculation, one pony of each group was euthanized
165 with an overdose of Natriumpentobarbital® (Kela, Hoogstraten, Belgium). After euthanasia,
166 different tissue samples were collected from the upper respiratory tract. Tissues from
167 slaughterhouse horses were collected and served as uninfected control samples. Per tissue,
168 two equal squares of 1 cm^2 were collected from both left and right side of the head. From
169 each side, one square was frozen immediately with (immunofluorescence) or without (virus
170 titration) methylcellulose medium (Methocel®MC, Sigma-Aldrich, St. Louis, MO, USA) at -
171 70°C. To determine viral replication, 20% suspensions of collected tissues were made and

titrated on RK13 cells. Titers of infected tissues were determined after 7 days by means of Reed and Muench's formula (Reed and Muench, 1938).

The experimental design was approved by the local ethical committee of the Faculty of Veterinary Medicine.

Quantification and characterization of individual infected cells in tissues of the upper respiratory tract

Immunofluorescent double stainings were used to quantify and characterize individual infected cells in tissues that were EHV1-positive after titration on RK13 cells. First, cryosections (16 µm) were incubated with either monoclonal antibody (mAb) HT23A, DH59B or 1.9/3.2 (VMRD Inc, Pullman, WA, USA) against CD5 (T-lymphocytes), CD172a (cells from the monocyte lineage, CML) or IgM (B-lymphocytes) respectively, and subsequently incubated with Texas Red®-labeled goat anti-mouse Abs (Molecular Probes, Eugene, OR, USA). Epithelial cells were identified based on the pancytokeratin marker MNF116 (Abcam, Cambridge, UK) and/or morphological features. Second, viral EHV1 proteins were stained by incubation with biotinylated polyclonal horse anti-EHV1 IgG (van der Meulen et al., 2000), followed by streptavidin-FITC® (Molecular Probes, Eugene, OR, USA). As controls, (i) stainings were performed on uninfected tissue and (ii) isotype control antibodies were included. All cryosections were analyzed using confocal microscopy (Leica TCS SP2 Laser scanning spectral confocal system, Leica Microsystems GmbH, Wetzlar, Germany). Number and latitude of EHV1-induced plaques were calculated using the software program ImageJ. Latitude was used to evaluate plaque size and therefore the degree of cell-to-cell spread. In order to quantify infected cells in nasal septum, two main regions were taken into account, on the one hand regions with and on the other hand regions without plaques in the epithelium. These regions were then subdivided into three equal regions underneath the

epithelium: A, B and C for regions with epithelial plaques and D, E and F for regions without epithelial plaques (Fig 2A). For nasopharynx, tubal/nasopharyngeal tonsils and lymph nodes, subdivisions into different zones of functional importance were made (Fig 3A and 4A respectively). All regions were evaluated for the presence of plaques and/or individual infected cells. In addition, the total amount of infected cells (positive for staining with anti-EHV1 Abs), equine immune cells (positive for staining with the mAbs against immune cell markers) and infected equine immune cells (double positive) were determined.

Quantification and characterization of viremia

Heparinized blood samples were taken daily until euthanasia and peripheral blood mononuclear cells (PBMC) were isolated by density centrifugation on Ficoll-Paque, according to manufacturer's instructions (Pharmacia Biotech AB, Uppsala, Sweden). To determine the magnitude of viremia, co-cultivation of PBMC on RK13 cells was performed as previously described (van der Meulen et al., 2003b). Remaining PBMC were resuspended in RPMI supplemented with 30% FCS and 20% Dimethyl Sulfoxide (DMSO) and frozen in liquid nitrogen for later examination to identify the nature of infected cells. Hereby, a double immunofluorescence staining was performed on acetone-fixed cell smears of PBMC. EHV1 expression was detected using a biotinylated polyclonal horse anti-EHV1 IgG (van der Meulen et al., 2003b), followed by streptavidin-FITC®. The identity of infected cells was determined using the mAbs HT23A, DH59B or 1.9/3.2, as described above, followed by the incubation with Texas Red®-labeled goat anti-mouse Abs. Samples were analyzed using confocal laser scanning microscopy.

Results

EHV-status of the ponies before inoculation

The inclusion criterium for ponies used in this study was a complete absence of EHV-specific antibodies by either SN-test (<2) or IPMA (<10). In addition, during the 4-week observation period prior to the experiment, (i) no raise in temperature was noted, (ii) no EHV-specific antibodies were detected, and (iii) no virus was isolated from nasopharyngeal swabs. The use of naïve horses is an important tool to minimize variation in clinical and virological outcome due to differences in immunological status (Cornick et al., 1990; Heldens et al., 2001; Matsumura et al., 1996).

Experimental inoculation with either strain induces fever and upper respiratory tract disease in ponies

All ponies developed fever upon EHV1 inoculation with exception of the two ponies that were euthanized 24 hours post inoculation (hpi). Fever started at 48 hpi for the neurovirulent strain (5/5 animals) and at 36 (3/5 animals) or 48 hpi (2/5 animals) for the non-neurovirulent strain. High temperatures lasted for the complete observation period, with peak temperatures of 40.7°C for the neurovirulent strain and 40.1°C for the non-neurovirulent strain. Serous nasal discharge was noted after inoculation with both strains, starting at 1 day post inoculation (dpi). A transition to purulent nasal discharge was seen in both groups from 3 dpi. Breathing problems, consisting of tachypnea or coughing, were observed in two ponies of each group. Swelling of mandibular lymph nodes was observed in the majority of the ponies and occurred from 1 dpi in 2/6 animals inoculated with a neurovirulent strain and in 4/6 animals inoculated with a non-neurovirulent strain. Painful retropharyngeal lymph nodes were noted in 5/6 ponies inoculated with a non-neurovirulent strain, in contrast to only 2 ponies inoculated with a neurovirulent strain. None of the ponies showed neurological signs, irrespective of the strain used for inoculation. The latter is not too unexpected, as the

incubation period of EHV1-induced neurological disorders is normally 6 to 10 days (Edington et al., 1986; Jackson et al., 1977; Mumford and Edington, 1980). Moreover, nervous system disorders have been described to occur more frequently in older horses and certain breeds (Garre et al., 2009; Goehring et al., 2006; Greenwood and Simson, 1980; Jackson et al., 1977; McCartan et al., 1995).

Experimental inoculation with either strain results in nasal shedding and viral replication in the upper respiratory tract, but differences were observed in the preferential epithelial replication site between strains

When evaluating nasal shedding, by titrations of nasal swab samples, five out of six ponies inoculated with the neurovirulent strain shed virus from 1 dpi, with a peak excretion at 2 dpi (Fig 1). Nasal shedding then slowly decreased until 7 dpi. For the non-neurovirulent strain, 6 out of 6 ponies shed virus at 1 dpi, reaching a peak at 2 dpi with remaining high titers until 7 dpi (Fig 1).

Next, different tissue samples were collected from the upper respiratory tract of one pony per group per day for viral titrations. Virus could not be isolated from any tissue at 1 dpi for the neurovirulent strain, but was found in the nasopharynx of ponies inoculated with the non-neurovirulent strain (Fig 2). From 2 dpi, virus was mainly recovered from different parts of the nasal septum and the nasopharynx for both strains (Fig 2). Septum and nasopharynx remained positive for EHV1 until 7 dpi, with the exception of day 5 for the neurovirulent strain where no virus was detected in the nasopharynx (Fig 2) and day 4 for the non-neurovirulent strain where the distal nasal septum was negative (Fig 2). No difference in virus titers could be noticed in the nasal septum, but titers found in the nasopharynx seemed to be higher after inoculation with the non-neurovirulent strain of EHV1 compared to the neurovirulent strain (Fig 2). However, because of the limited number of animals used, we

should be careful to draw any conclusions based on these results. Virus was also found in lymphoid tissues such as the tubal and nasopharyngeal tonsils and mandibular lymph nodes (Fig 2). In general, titers found in tubal and nasopharyngeal tonsils (Fig 2) were higher for the non-neurovirulent strain. Titers detected in mandibular lymph nodes started rising from 3 dpi (neurovirulent strain) or 4 dpi (non-neurovirulent strain), and at 7dpi, mandibular lymph nodes were positive for the non-neurovirulent strain only (Fig 2). EHV1 could also be isolated for both strains at different time points pi from the ethmoid, the cranial part of the trachea and 3 different tonsils (data not shown).

Finally, replication of EHV1 was evaluated in the epithelium of different tissues of the upper respiratory tract by immunofluorescence. Hereby, EHV1-induced plaques were analyzed and plaque latitudes measured. In the epithelium of the entire nasal septum, EHV1-induced plaques were seen at different time points pi for both strains (Fig 3A). These plaques were defined as groups of infected epithelial cells. Since results for proximal, intermedial and distal nasal septum were virtually identical, only results for the intermedial nasal septum are shown. Plaques were not present in the epithelium at 0 and 1 dpi (Fig 3A). However, individual infected cells were observed at 1 dpi, which were identified as $CD172a^{+}$ cells, as determined by the marker DH59B, or epithelial cells, as determined by the pancytokeratin marker (data not shown). For the neurovirulent strain, EHV1-induced plaques were observed in the epithelium of the nasal mucosa starting from 2 till 7 dpi (Fig 3A). At 2, 3 and 4 dpi, these plaques consisted of epithelial cells and rarely one or two $CD172a^{+}$ cells. From 5 dpi, EHV1-positive cells became separated from the basement membrane (BM) and these cells were exclusively positive for the DH59B marker which identifies cells of the monocytic lineage (CML) (Fig 3A). This observation was not seen in ponies inoculated with a non-neurovirulent strain. There, plaques were present in the epithelium of the nasal mucosa and nasopharynx from 2 till 7 dpi (Fig 3A & B). These plaques consisted of epithelial cells and

rarely some CD172a$^+$ cells, but no separation of EHV1-positive cells was observed (Fig 3A). No differences were observed in both number (data not shown) and size (Fig 3A) of EHV1-induced plaques in the intermedial nasal mucosa at different time points pi for both strains. In the epithelium of the nasopharynx, plaques could be found for the non-neurovirulent strain from 2 till 7 dpi, with the exception of 4 dpi (Fig 3B). In contrast, no plaques were found for the neurovirulent strain in the nasopharyngeal epithelium, with the exception of one small plaque at 3 dpi (Fig 3B). Interestingly, plaques were not able to cross the BM at any time point pi, but single EHV1-infected cells could be noticed in the connective tissue from 1 dpi.

Taken together, these results show that EHV1 infection results in nasal shedding and replication in several tissues of the upper respiratory tract, irrespective of its neuropathogenic potential. However, whereas both types of EHV1 replicate equally in the epithelium of the nasal mucosa, replication in the nasopharynx was limited to non-neurovirulent EHV1.

Neurovirulent EHV1 uses mainly CD172a$^+$ cells as carrier cells in tissues of the upper respiratory tract, whereas non-neurovirulent EHV1 shows a tropism for both CD172a$^+$ cells and CD5$^+$ cells

As mentioned before, EHV1-induced plaques never crossed the BM, irrespective of the strain used. However, individual infected cells were observed in the underlying connective tissue and the total number was 3-7 times lower with non-neurovirulent EHV1 compared to neurovirulent EHV1. To identify the nature of these cells, cryosections of tissues were made and double immunofluorescence stainings were performed.

Nasal septum. In the connective tissue of the nasal septum, no differences were observed in the total amount of infected cells present beneath epithelium with plaques or without plaques, with the exception of 5 and 7 dpi for the neurovirulent strain, where a

marked increase in infected cells was observed in region A (Fig 4). Such increase was not seen in the regions located underneath epithelium without plaques (Fig 4).

Nasopharynx. EHV1-infected cells were present in the connective tissue of the nasopharynx from 1 till 7 dpi, irrespective of the strain used, however, the localization of these cells appeared to be strain-dependent (Fig 5). Whereas for the neurovirulent strain, single infected cells were mainly found in epithelium (region A) and connective tissue (region B), single infected cells were located in connective tissue (region B) and lymphocyte aggregates (region C) for the non-neurovirulent strain (Fig 5).

Tubal and nasopharyngeal tonsils. For both EHV1 strains, single infected cells were observed starting from 2 dpi (Fig 6). They were mostly present in the connective tissue underneath the epithelium (region B) and lymphocyte aggregates (region C, Fig 6), but single infected cells could also be observed in epithelium/fundus (region A), deeper connective tissue (region D), blood vessels (region E) and glands (region F) (Fig 6).

Mandibular lymph nodes. For the neurovirulent strain, most of the infected cells were found in the marginal sinus of the mandibular lymph nodes (region C, Fig 7). Their number increased until 4 dpi and rapidly decreased afterwards, with rarely any infected cells left at 7 dpi. Furthermore, infected cells were also observed in the capsule and trabecula (region A), the medulla (region F) and in fewer amounts in vessels of the capsule and the cortical nodules (regions B and D, Fig 7). In these regions a peak number of infected cells was observed at 4 and 5 dpi (Fig 7). For the non-neurovirulent strain, single cells were only found from 4 till 7 dpi and were mostly found in the marginal sinus (region C) and medulla (region F) (Fig 7).

Immunofluorescence stainings, using mAbs against immune cell surface markers showed that in all tissues of the upper respiratory tract, infected cells were largely $CD172a^+$ CML, followed by a slightly lower amount of infected $CD5^+$ lymphocytes when the

neurovirulent EHV1 strain was used for inoculation (Table I). These results were very similar to what was observed with the non-neurovirulent strain, although a more substantial amount of infected $CD5^+$ lymphocytes was observed in these different tissues of the upper respiratory tract (Table I). IgM^+ lymphocytes were always present, but rarely infected with the exception of the mandibular (Table I) and retropharyngeal (data not shown) lymph nodes, were these cells were an important target cell type for both strains.

Ponies became viremic upon experimental inoculation with either strain, and $CD172a^+$ cells were the most important carrier cells in the blood

Transmission of EHV1 from PBMC to susceptible RK13 cells, as determined by co-cultivation, was observed in 5 out of 6 ponies upon experimental inoculation with neurovirulent EHV1 (Fig 8). No differences in the amount of infected PBMC was noted, except for one pony, which showed a higher level of viremia at 4 and 5 dpi compared to the other infected ponies (Fig 8). For the non-neurovirulent strain, viremia was observed in all six infected ponies, with no differences in magnitude for the first 4 dpi (Fig A). However, at day 5 and 7 pi, the non-neurovirulent strain seemed to retain a higher viremia level then the neurovirulent strain, but due to the low amount of animals left at those days, no conclusions could be drawn (Fig 8).

In addition, around 2×10^7 mononuclear cells for each strain were analyzed by confocal microscopy to detect infected cells and further characterize their nature. These cells were a mixture of PBMC from three ponies collected at 2, 3 and 4 dpi. For the neurovirulent strain, fourteen EHV1-infected cells were found and eleven were characterized as $CD172a^+$ cells (78.5%), whereas three were $CD5^+$ (21.5%). No infected B-lymphocytes were found. For the non-neurovirulent strain, nine EHV1-infected cells were identified, consisting of seven

370 CD172a^{+} cells (77.8%), one CD5^{+} T-lymphocyte (11.0%) and one cell remained unidentified.
371 Also here, no infected B-lymphocytes were found.
372 These data indicate that CD172a^{+} cells appear to be the main target cell during EHV1-
373 induced viremia, irrespective of the neuropathogenicity of EHV1.
374

Discussion

Despite several studies conducted on the pathogenesis of equine herpesvirus type 1 (EHV1), it still remains unclear how this virus invades the tissues of the upper respiratory tract and invades the deeper tissues to initiate a cell-associated viremia. Furthermore, two strains of EHV1 circulate in the field, namely non-neurovirulent and neurovirulent strains, the latter causing neurological disease, a severe condition which is poorly understood. In the present study, we used the two strains of EHV1 to gain more insight into the pathogenesis of these strains during the acute phase of infection in the upper respiratory tract *in vivo*. To this end, Shetland ponies were experimentally inoculated with either a non-neurovirulent or a neurovirulent EHV1 strain and upon euthanasia, several tissues from the upper respiratory tract were collected and analyzed.

It was found that EHV1 has different approaches to successfully establish an infection in the upper respiratory tract. Firstly, we observed that EHV1, irrespective of the strain, can replicate in the epithelium of the nasal septum and/or nasopharynx by means of virus-induced plaques. This replication appears to occur in a restricted way, as no increase in number or size of plaques was observed over time. In addition, a repulsion of EHV1-induced plaques was observed from 5 dpi onwards for the neurovirulent strain, and a decrease in plaque latitude was seen for the non-neurovirulent strain starting at day 3 pi. This reduction in replication might be attributed to the production of interferon (IFN), as (i) the presence of interferon in nasal secretions after experimental inoculation of horses with EHV1 has previously been described and (ii) peak concentrations of IFN-α were noted at day 4 and day 7 pi (Bridges and Edington, 1986; Edington et al., 1989). In the present study, IFN-α was also found in nasal swabs of experimentally infected ponies (data not shown), which further points towards the importance of IFN to limit EHV1 replication in the epithelium of the upper respiratory tract. Interestingly, even though the non-neurovirulent strain was able to replicate in a plaquewise

manner in the epithelium of the nasopharynx, no plaques could be observed at any time point pi in the nasopharynx after inoculation with the neurovirulent strain. As the epithelial structure of both tissues is identical, with the exception of the presence of lymphoid aggregates in the nasopharynx, the reason for this observation remains elusive. Another interesting observation for both EHV1 strains was that we were unable to observe EHV1-infected plaques under the basement membrane (BM) at any time point pi, indicating that EHV1 does not reach the underlying tissue by breaking down the BM. This is in striking contrast to previous findings with another and closely related alphaherpesvirus, pseudorabies virus (PRV), which has been shown to cross the BM in a plaque wise manner between 12 and 24 hpi in a porcine respiratory explant model (Glorieux et al., 2009). This indicates that different alphaherpesviruses may use different mechanisms to invade the underlying connective tissue. Indeed, whereas PRV was shown to break down the BM and replicates further in the underlying tissue in a plaquewise manner, our study with EHV1 demonstrated only single infected cells below the BM. This is in agreement with previous studies on EHV1, where the presence of single infected cells in tissues of the upper respiratory tract has been reported (Edington et al., 1986; Kydd et al., 1994). We could further demonstrate that these infected cells in the underlying tissue were immune cells (as discussed in more detail below), which makes it tempting to speculate that immune cells in the epithelium become infected with EHV1 and are responsible for transporting the virus to deeper connective tissue. Indeed, we did found EHV1-infected cells in the epithelium of nasal septum and/or nasopharynx, which were further characterized to belong to the monocytic lineage (CML) by using the cell surface maker CD172a. Not only differences concerning the identity of the EHV1-infected immune cells present in the underlying tissues were noticed between both strains, moreover, differences concerning there localization were also observed. When analyzing the identity of the single EHV1-infected cells in the connective tissue of nasal septum and nasopharynx,

425 several differences could be observed between the two EHV1 strains. Firstly, the total number
426 of infected cells in the nasal septum was 10 to 20 times higher for the neurovirulent strain
427 compared to the non-neurovirulent strain. Secondly, while individual infected cells in the
428 nasopharynx were mainly present in the connective tissue upon neurovirulent EHV1
429 inoculation, individual cells infected with the non-neurovirulent EHV1 seemed to migrate
430 deeper into the lymphoid follicles of the nasopharynx in a time wise manner. Thirdly,
431 $CD172a^+$ CML were the most important carrier cells for both neurovirulent and non-
432 neurovirulent EHV1, although these cells seemed to be more important for the neurovirulent
433 strain. In addition, both strains were able to infect $CD5^+$ T-lymphocytes, with a higher amount
434 of infected cells for the non-neurovirulent strain (Table I). When analyzing the data on the
435 identity of infected cells in lymphoid tissues of the upper respiratory tract, we again observed
436 that the most prominent target cells for EHV1 were $CD172a^+$ CML, irrespective of the strain
437 used. This is in line with previous studies, where EHV1-infected macrophages and
438 lymphoblasts were detected in lymph nodes after inoculation with EHV1 isolates from both
439 an aborted fetus and a paralyzed mare (Patel et al., 1982). Moreover, another EHV1
440 experimental inoculation study showed that lymphocytes, monocytes, macrophages and
441 plasma cells in interstitium and lymph nodes all expressed EHV1 antigens, as determined by
442 immunohistochemical staining using anti-EHV1 polyclonal Abs (Kydd et al., 1994). In the
443 present study, the majority of EHV1-positive cells was found in the marginal sinus of lymph
444 nodes. At those sites, transport is possible to extra follicular interdigitating cells in the lymph
445 node where both mature and virgin lymphocytes have access to antigen, hereby initiating
446 humoral immune responses (Tew et al., 1990). Surprisingly, and in contrast to what was
447 observed in nasal septum and nasopharynx, IgM^+ B-lymphocytes were also an important
448 target cell for EHV1. *In vitro* it has been previously shown that a 6- to 14-fold increase of
449 EHV1-infected peripheral blood mononuclear cells (PBMC) could be obtained after *in vitro*

450 stimulation with proliferating drugs such as pokeweed mitogen (PWM), concanavalin A
451 (ConA), phytohaemagglutinin (PHA), or ionomycin and phorbol dibutyrate (IONO/PDB)
452 (van der Meulen et al., 2001). Together with the fact that B-lymphocytes are known to
453 undergo extensive proliferation in lymphoid follicles (Fu and Chaplin, 1999), we would like
454 to reason that the elevated percentage of EHV1-infected B-lymphocytes observed in
455 lymphoid tissues, is due to the proliferation stage of these immune cells.

456 The onset of a cell-associated viremia could be detected as early as one day after
457 experimental inoculation with EHV1, indicating that EHV1-infected cells can enter the blood
458 stream very rapidly. Moreover, we identified these EHV1-positive cells as mainly $CD172a^+$
459 CML. Despite the fact that only 14 infected cells were found, we strongly feel that this low
460 number is of relevance, as it is known that EHV1-induced viremia is generally very low with
461 numbers ranging from 1 to 10 positive cells/0.8 x 10^7 PBMC (van der Meulen et al., 2006).
462 Combining the results on the identity of EHV1-infected cells in the connective tissues of the
463 primary port of entry, the upper respiratory tract, with the results on the identity of the EHV1-
464 infected cells in the blood, we would like to hypothesize that the $CD172a^+$ cells we observed
465 could be dendritic cells (DCs). The reasoning behind such hypothesis is as follows. The
466 marker DH59B that was used in the present study to identify $CD172a^+$ cells is a pan
467 granulocyte/monocyte marker which has been used in several studies as a DC marker (Ahn et
468 al., 2002; Tumas et al., 1994). In addition, there is evidence indicating that local tissue DCs
469 are able to re-enter the bloodstream, which might facilitate the spread of pathogens from
470 tissue to tissue, carried by DCs serving as Trojan horses (Randolph et al., 2008). Finally, DCs
471 have been shown to play an important role during the pathogenesis of alphaherpesviruses in
472 general (Bosnjak et al., 2005; Novak and Peng, 2005; Pollara et al., 2005), and for EHV1 in
473 specific, both murine and equine blood-derived DCs are susceptible to EHV1 *in vitro* (Siedek
474 et al., 1999; Steinbach et al., 1998). Unfortunately, little is known about equine DCs in

general and mucosal DCs in specific in this species, and more research is needed to elucidate the role of DCs in EHV1 infection and/or other viral infections in equines. Regardless, the results presented here are in striking contrast to another *in vivo* study, where mainly blood T-lymphocytes were found to harbor EHV1 (Scott et al., 1983). However, in the latter study, leukocyte populations were solely separated by glass-bead columns and no direct characterization was performed. A possible explanation for the discrepancy between cell types infected during cell-associated viremia could be the strain used. In a previous study an American strain, isolated from an aborted fetus, was used (Scott et al., 1983) whereas in the present study, we used two Belgian EHV1 strains. Surprisingly, we observed $CD172a^+$ cells as the main carrier cell type for both the neurovirulent and the non-neurovirulent strain, indicating that the EHV1 strain does not seem to correlate with a difference in cell tropism during viremia. This is again in contrast to another study, where a difference in leukocyte tropism between neuro- and non-neurovirulent EHV1 strains has been demonstrated (Goodman et al., 2007). Hereby it was observed that the EHV1 strain Ab4, which has the neuropathogenic genotype, mainly infected $CD4^+$ lymphocytes, whereas mutating this strain into the non-neuropathogenic genotype resulted in a preferential infection of monocytes and B-cells. However, these experiments were performed with *in vitro* infected PBMC, which most likely explains the discrepancy with our *in vivo* data.

Conclusion

Based on all the observations presented in this study, we would like to propose following model on the pathogenesis of different EHV1 strains in the upper respiratory tract. Upon infection, EHV1 replication in epithelial cells of the nasal septum, and nasopharynx for the non-neurovirulent strain, results in a productive infection with plaque formation and nasal virus shedding. This nasal shedding allows for transmission of virus to susceptible contact

animals and ensures that EHV1 can persist in the equine population. This productive infection in epithelial cells, however, is self-limiting, most likely because of IFN-α production. In addition, EHV1 seems to cross the BM through the help of $CD172a^+$ carrier cells, probably mucosal dendritic cells. We postulate that these carrier cells which become infected with EHV1 can transport the virus across the basement membranes and through connective tissues in the direction of vascular endothelial cells on the one hand and lymphatic epithelium on the other hand. As a result, a cell-associated viremia is originated, together with a migration of infected immune cells to local lymph nodes, hereby initiating the start of a specific immune response. Although not observed in this study, the higher potential of the neurovirulent strain to infect large amounts of carrier cells, could lead to a prolonged viremia, with a higher risk of developing nervous system disorders.

Despite the fact that only a limited number of animals could be included in this experiment, we still feel that this paper revealed important new insights about the pathogenesis of neurovirulent and non-neurovirulent strains in the acute phase of infection in horses.

Acknowledgements

This research was supported by the Institute for the promotion of Innovation through Science and Technology in Flanders (IWT-Vlaanderen). The authors like to thank C. Boone and N. Monteiro for titrations, and C. Bracke for isolation of PBMC and performing SN-tests.

Conflict of interest

None of the authors of this paper has a financial or personal relationship with other people or organisations that could inappropriately influence or bias the content of the paper.

References

525 Ahn, J.S., Konno, A., Gebe, J.A., Aruffo, A., Hamilton, M.J., Park, Y.H., Davis, W.C., 2002,
526 Scavenger receptor cysteine-rich domains 9 and 11 of WC1 are receptors for the WC1
527 counter receptor. J Leukoc Biol 72, 382-390.
528 Allen, G.P., Breathnach, C.C., 2006, Quantification by real-time PCR of the magnitude and
529 duration of leucocyte-associated viraemia in horses infected with neuropathogenic vs.
530 non-neuropathogenic strains of EHV-1. Equine Vet J 38, 252-257.
531 Allen, G.P., Bryans, J.T., 1986, Molecular epizootiology, pathogenesis, and prophylaxis of
532 equine herpesvirus-1 infections. Prog Vet Microbiol Immunol 2, 78-144.
533 Bosnjak, L., Jones, C.A., Abendroth, A., Cunningham, A.L., 2005, Dendritic cell biology in
534 herpesvirus infections. Viral Immunol 18, 419-433.
535 Bridges, C.G., Edington, N., 1986, Innate immunity during Equid herpesvirus 1 (EHV-1)
536 infection. Clin Exp Immunol 65, 172-181.
537 Cornick, J., Martens, J., Martens, R., Crandell, R., McConnell, S., Kit, S., 1990, Safety and
538 efficacy of a thymidine kinase negative equine herpesvirus-1 vaccine in young horses.
539 Can J Vet Res 54, 260-266.
540 Edington, N., Bridges, C.G., Griffiths, L., 1989, Equine interferons following exposure to
541 equid herpesvirus-1 or -4. J Interferon Res 9, 389-392.
542 Edington, N., Bridges, C.G., Patel, J.R., 1986, Endothelial cell infection and thrombosis in
543 paralysis caused by equid herpesvirus-1: equine stroke. Arch Virol 90, 111-124.
544 Fu, Y.X., Chaplin, D.D., 1999, Development and maturation of secondary lymphoid tissues.
545 Annu Rev Immunol 17, 399-433.
546 Garre, B., Gryspeerdt, A., Croubels, S., De Backer, P., Nauwynck, H., 2009, Evaluation of
547 orally administered valacyclovir in experimentally EHV1-infected ponies. Vet
548 Microbiol 135, 214-221.

549 Glorieux, S., Favoreel, H.W., Meesen, G., de Vos, W., Van den Broeck, W., Nauwynck, H.J.,
550 2009, Different replication characteristics of historical pseudorabies virus strains in
551 porcine respiratory nasal mucosa explants. Vet Microbiol 136, 341-346.
552 Goehring, L.S., van Winden, S.C., van Maanen, C., Sloet van Oldruitenborgh-Oosterbaan,
553 M.M., 2006, Equine herpesvirus type 1-associated myeloencephalopathy in The
554 Netherlands: a four-year retrospective study (1999-2003). J Vet Intern Med 20, 601-
555 607.
556 Goodman, L.B., Loregian, A., Perkins, G.A., Nugent, J., Buckles, E.L., Mercorelli, B., Kydd,
557 J.H., Palu, G., Smith, K.C., Osterrieder, N., Davis-Poynter, N., 2007, A point mutation
558 in a herpesvirus polymerase determines neuropathogenicity. PLoS Pathog 3, 1583-
559 1592.
560 Greenwood, R.E., Simson, A.R., 1980, Clinical report of a paralytic syndrome affecting
561 stallions, mares and foals on a thoroughbred studfarm. Equine Vet J 12, 113-117.
562 Heldens, J.G., Hannant, D., Cullinane, A.A., Prendergast, M.J., Mumford, J.A., Nelly, M.,
563 Kydd, J.H., Weststrate, M.W., van den Hoven, R., 2001, Clinical and virological
564 evaluation of the efficacy of an inactivated EHV1 and EHV4 whole virus vaccine
565 (Duvaxyn EHV1,4). Vaccination/challenge experiments in foals and pregnant mares.
566 Vaccine 19, 4307-4317.
567 Jackson, T.A., Osburn, B.I., Cordy, D.R., Kendrick, J.W., 1977, Equine herpesvirus 1
568 infection of horses: studies on the experimentally induced neurologic disease. Am J
569 Vet Res 38, 709-719.
570 Kydd, J.H., Smith, K.C., Hannant, D., Livesay, G.J., Mumford, J.A., 1994, Distribution of
571 equid herpesvirus-1 (EHV-1) in the respiratory tract of ponies: implications for
572 vaccination strategies. Equine Vet J 26, 466-469.

573 Matsumura, T., O'Callaghan, D.J., Kondo, T., Kamada, M., 1996, Lack of virulence of the
574 murine fibroblast adapted strain, Kentucky A (KyA), of equine herpesvirus type 1
575 (EHV-1) in young horses. Vet Microbiol 48, 353-365.
576 McCartan, C.G., Russell, M.M., Wood, J.L., Mumford, J.A., 1995, Clinical, serological and
577 virological characteristics of an outbreak of paresis and neonatal foal disease due to
578 equine herpesvirus-1 on a stud farm. Vet Rec 136, 7-12.
579 Mumford, J.A., Edington, N., 1980, EHV1 and equine paresis. Vet Rec 106, 277.
580 Novak, N., Peng, W.M., 2005, Dancing with the enemy: the interplay of herpes simplex virus
581 with dendritic cells. Clin Exp Immunol 142, 405-410.
582 Nugent, J., Birch-Machin, I., Smith, K.C., Mumford, J.A., Swann, Z., Newton, J.R., Bowden,
583 R.J., Allen, G.P., Davis-Poynter, N., 2006, Analysis of equid herpesvirus 1 strain
584 variation reveals a point mutation of the DNA polymerase strongly associated with
585 neuropathogenic versus nonneuropathogenic disease outbreaks. J Virol 80, 4047-4060.
586 Ostlund, E.N., 1993, The equine herpesviruses. Vet Clin North Am Equine Pract 9, 283-294.
587 Patel, J.R., Edington, N., Mumford, J.A., 1982, Variation in cellular tropism between isolates
588 of equine herpesvirus-1 in foals. Arch Virol 74, 41-51.
589 Pollara, G., Kwan, A., Newton, P.J., Handley, M.E., Chain, B.M., Katz, D.R., 2005, Dendritic
590 cells in viral pathogenesis: protective or defective? Int J Exp Pathol 86, 187-204.
591 Randolph, G.J., Ochando, J., Partida-Sanchez, S., 2008, Migration of dendritic cell subsets
592 and their precursors. Annu Rev Immunol 26, 293-316.
593 Reed, L.J., Muench, H., 1938, A simple method of estimating fifty per cent endpoints. Am J
594 Hyg 27, 493-497.
595 Scott, J.C., Dutta, S.K., Myrup, A.C., 1983, In vivo harboring of equine herpesvirus-1 in
596 leukocyte populations and subpopulations and their quantitation from experimentally
597 infected ponies. Am J Vet Res 44, 1344-1348.

598 Siedek, E.M., Whelan, M., Edington, N., Hamblin, A., 1999, Equine herpesvirus type 1
599 infects dendritic cells in vitro: stimulation of T lymphocyte proliferation and
600 cytotoxicity by infected dendritic cells. Vet Immunol Immunopathol 67, 17-32.
601 Steinbach, F., Borchers, K., Ricciardi-Castagnoli, P., Ludwig, H., Stingl, G., Elbe-Burger, A.,
602 1998, Dendritic cells presenting equine herpesvirus-1 antigens induce protective anti-
603 viral immunity. J Gen Virol 79, 3005-3014.
604 Stierstorfer, B., Eichhorn, W., Schmahl, W., Brandmuller, C., Kaaden, O.R., Neubauer, A.,
605 2002, Equine herpesvirus type 1 (EHV-1) myeloencephalopathy: a case report. J Vet
606 Med B Infect Dis Vet Public Health 49, 37-41.
607 Tew, J.G., Kosco, M.H., Burton, G.F., Szakal, A.K., 1990, Follicular dendritic cells as
608 accessory cells. Immunol Rev 117, 185-211.
609 Tumas, D.B., Brassfield, A.L., Travenor, A.S., Hines, M.T., Davis, W.C., McGuire, T.C.,
610 1994, Monoclonal antibodies to the equine CD2 T-lymphocyte marker, to a pan-
611 granulocyte monocyte marker and to a unique pan-B lymphocyte marker.
612 Immunobiology 192, 48-64.
613 Van de Walle, G.R., Goupil, R., Wishon, C., Damiani, A., Perkins, G.A., Osterrieder, N.,
614 2009, A Single-Nucleotide Polymorphism in a Herpesvirus DNA Polymerase Is
615 Sufficient to Cause Lethal Neurological disease. J Infect Dis 200, 20-25.
616 van der Meulen, K., Caij, B., Pensaert, M., Nauwynck, H., 2006, Absence of viral envelope
617 proteins in equine herpesvirus 1-infected blood mononuclear cells during cell-
618 associated viremia. Vet Microbiol 113, 265-273.
619 van der Meulen, K., Vercauteren, G., Nauwynck, H., Pensaert, M., 2003a, A local epidemic
620 of equine herpesvirus 1-induced neurological disorders in Belgium. Vlaams Diergen
621 Tijds 72, 366-372.

van der Meulen, K.M., Nauwynck, H.J., Buddaert, W., Pensaert, M.B., 2000, Replication of equine herpesvirus type 1 in freshly isolated equine peripheral blood mononuclear cells and changes in susceptibility following mitogen stimulation. J Gen Virol 81, 21-25.

van der Meulen, K.M., Nauwynck, H.J., Pensaert, M.B., 2001, Mitogen stimulation favours replication of equine herpesvirus-1 in equine blood mononuclear cells by inducing cell proliferation and formation of close intercellular contacts. J Gen Virol 82, 1951-1957.

van der Meulen, K.M., Nauwynck, H.J., Pensaert, M.B., 2003b, Absence of viral antigens on the surface of equine herpesvirus-1-infected peripheral blood mononuclear cells: a strategy to avoid complement-mediated lysis. J Gen Virol 84, 93-97.

van Maanen, C., 2002, Equine herpesvirus 1 and 4 infections: an update. Vet Q 24, 58-78.

Figure legends

Figure 1. Nasal viral shedding. Ponies were inoculated with a neurovirulent or a non-neurovirulent strain of EHV1. At 0, 1, 2, 3, 4, 5 and 7 days post inoculation (dpi), nasopharyngeal swabs were collected and titrated as described in material and methods.

Figure 2. Viral replication in different tissues of the upper respiratory tract. Ponies were inoculated with either neurovirulent or non-neurovirulent EHV1 and euthanized at 0, 1, 2, 3, 4, 5 and 7 days post inoculation (dpi). Different tissues were collected and titrated as described in materials and methods.

Figure 3. Plaque formation in epithelium of intermedial nasal septum and nasopharynx. Ponies were inoculated with either neurovirulent or non-neurovirulent EHV1 and euthanized

at 0, 1, 2, 3, 4, 5 and 7 days post inoculation (dpi). Tissues of the intermedial part of the nasal septum (A) and nasopharynx (B) were collected and latitude of plaques were determined. For each tissue, ten consecutive sections were made and the total number of individual plaques was determined. This number is presented above the relevant histogram. The largest measurement of latitude of each individual plaque was used to determine plaque latitude. The sum was used to calculate the mean plaque latitude ± SEM. Representative immunofluorescence pictures of EHV1-induced plaques in the intermedial nasal septum are shown for neurovirulent or non-neurovirulent EHV1 for each dpi. BM: basement membrane, objective 20x**,** NI: non-infected epithelial cells.

Figure 4. Quantification and identification of single EHV1-infected cells in different zones of the intermedial nasal septum for neurovirulent and non-neurovirulent strains. Every tenth section of a serially sectioned block of tissue was collected. Ten sections were analysed for each cell marker separately, giving a total number of 30 sections. The total number of infected cells present in the intermedial nasal septum per zone and per day, is shown in the upper right table. The results for the identification of single infected cells are shown in the lower graphs and are represented as the mean of ten sections ± SEM. ROI: region of interest.

Figure 5. Quantification and identification of single EHV1-infected cells in different zones of the nasopharynx for neurovirulent and non-neurovirulent strains. Every tenth section of a serially sectioned block of tissue was collected. Ten sections were analysed for each cell marker separately, giving a total number of 30 sections. The total number of infected cells present in the nasopharynx per zone and per day, is shown in the upper right table. The

results for the identification of single infected cells are shown in the lower graphs and are represented as the mean of ten sections ± SEM. ROI: region of interest.

Figure 6. Quantification and identification of single EHV1-infected cells in different zones of the tubal and nasopharyngeal tonsils for neurovirulent and non-neurovirulent strains. Every tenth section of a serially sectioned block of tissue was collected. Ten sections were analysed for each cell marker separately, giving a total number of 30 sections. The total number of infected cells present in the tubal and nasopharyngeal tonsils per zone and per day, is shown in the upper right table. The results for the identification of single infected cells are shown in the lower graphs and are represented as the mean of ten sections ± SEM. ROI: region of interest.

Figure 7. Quantification and identification of single EHV1-infected cells in different zones of the mandibular lymph node for neurovirulent and non-neurovirulent strains. Every tenth section of a serially sectioned block of tissue was collected. Ten sections were analysed for each cell marker separately, giving a total number of 30 sections. The total number of infected cells present in the mandibular lymph node per zone and per day, is shown in the upper right table. The results for the identification of single infected cells are shown in the lower graphs and are represented as the mean of ten sections ± SEM. ROI: region of interest.

Figure 8. Quantification of viremia for neurovirulent and non-neurovirulent strains. Ponies were inoculated with a neurovirulent or a non-neurovirulent strain of EHV1. At 0, 1, 2, 3, 4, 5 and 7 days post inoculation (dpi), blood samples were collected and cocultivation of PBMC was performed as mentioned in materials and methods.

Table I. Percentage of marker positive EHV1-infected individual cells in different tissues of the upper respiratory tract

Region of interest	Percentage of marker positive EHV1-infected individual cells					
	Neurovirulent strain			Non-neurovirulent strain		
	CD172a$^+$	CD5$^+$	IgM$^+$	CD172a$^+$	CD5$^+$	IgM$^+$
Nasal septum	53.4 ± 22,8	16.2 ± 11.7	0.3 ± 0.8	43.9 ± 12.8	23.6 ± 8.6	0
Nasopharynx	69.5 ± 20.7	0	8.3 ± 20.4	37.9 ± 35.5	13.6 ± 5.7	1.1 ± 2.7
Tubal and nasopharyngeal tonsils	66.4 ± 20.7	11.2 ± 12.8	4.8 ± 5.6	28.7 ± 3.6	21.2 ± 5.9	0.5 ± 1.0
Mandibular lymph nodes	71.3 ± 17.9	7.3 ± 9.5	8.3 ± 8.8	42.6 ± 21	26.7 ± 5.7	7.7 ± 10.8

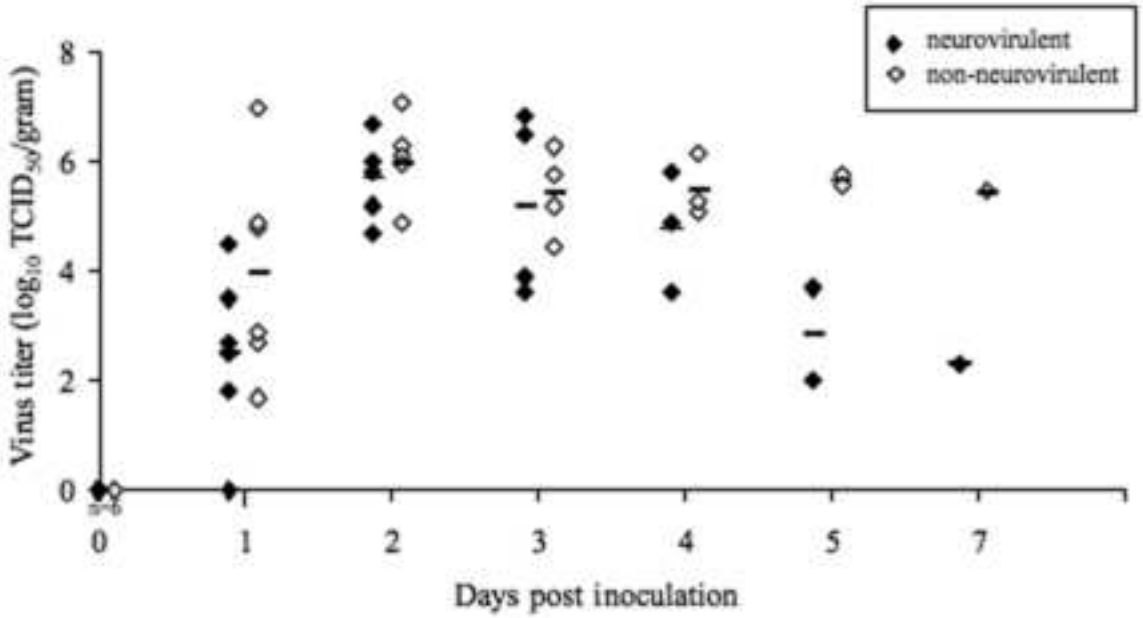

Fig 1 Gryspeerdt *et al.*

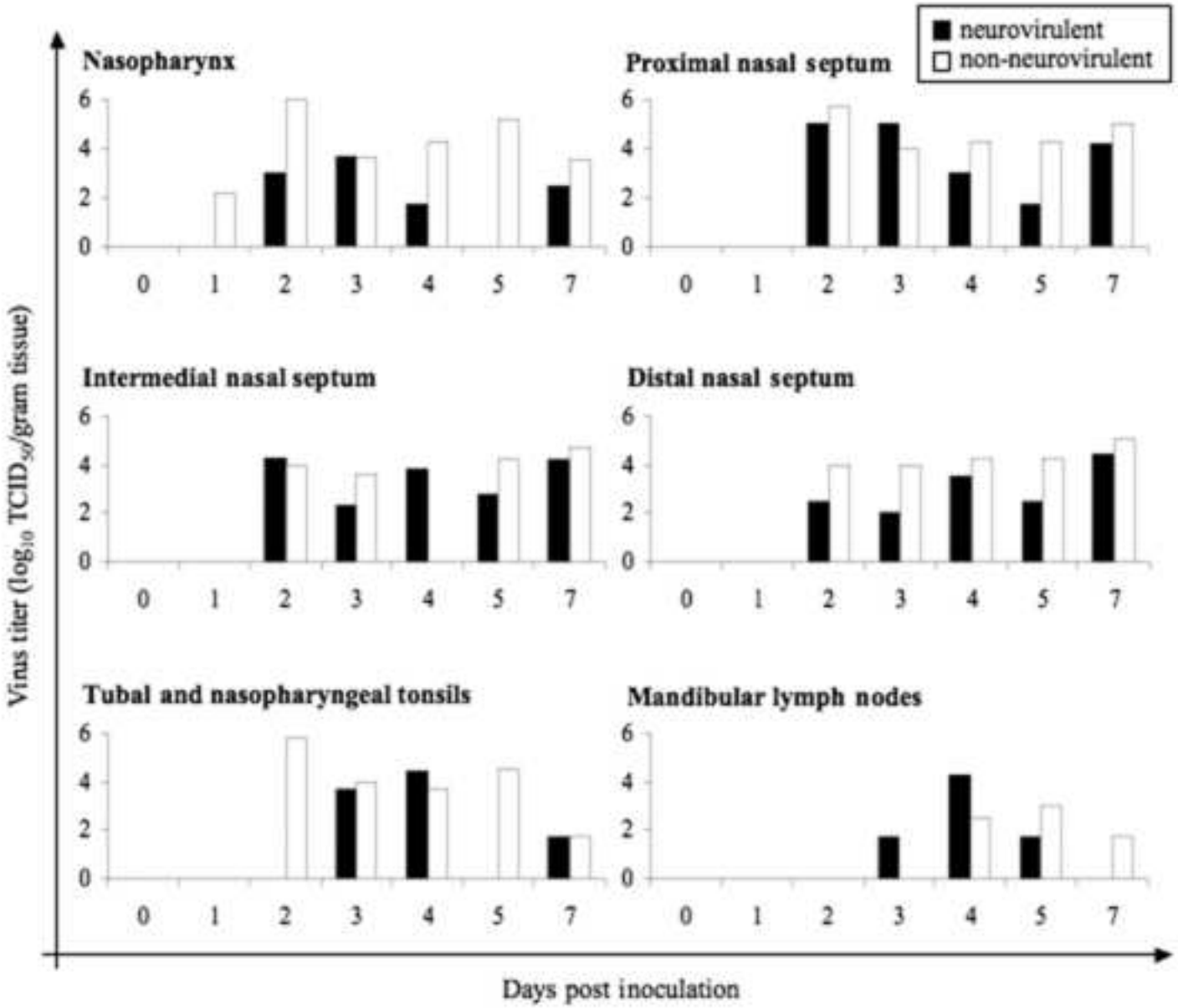

Fig 2 Gryspeerdt *et al.*

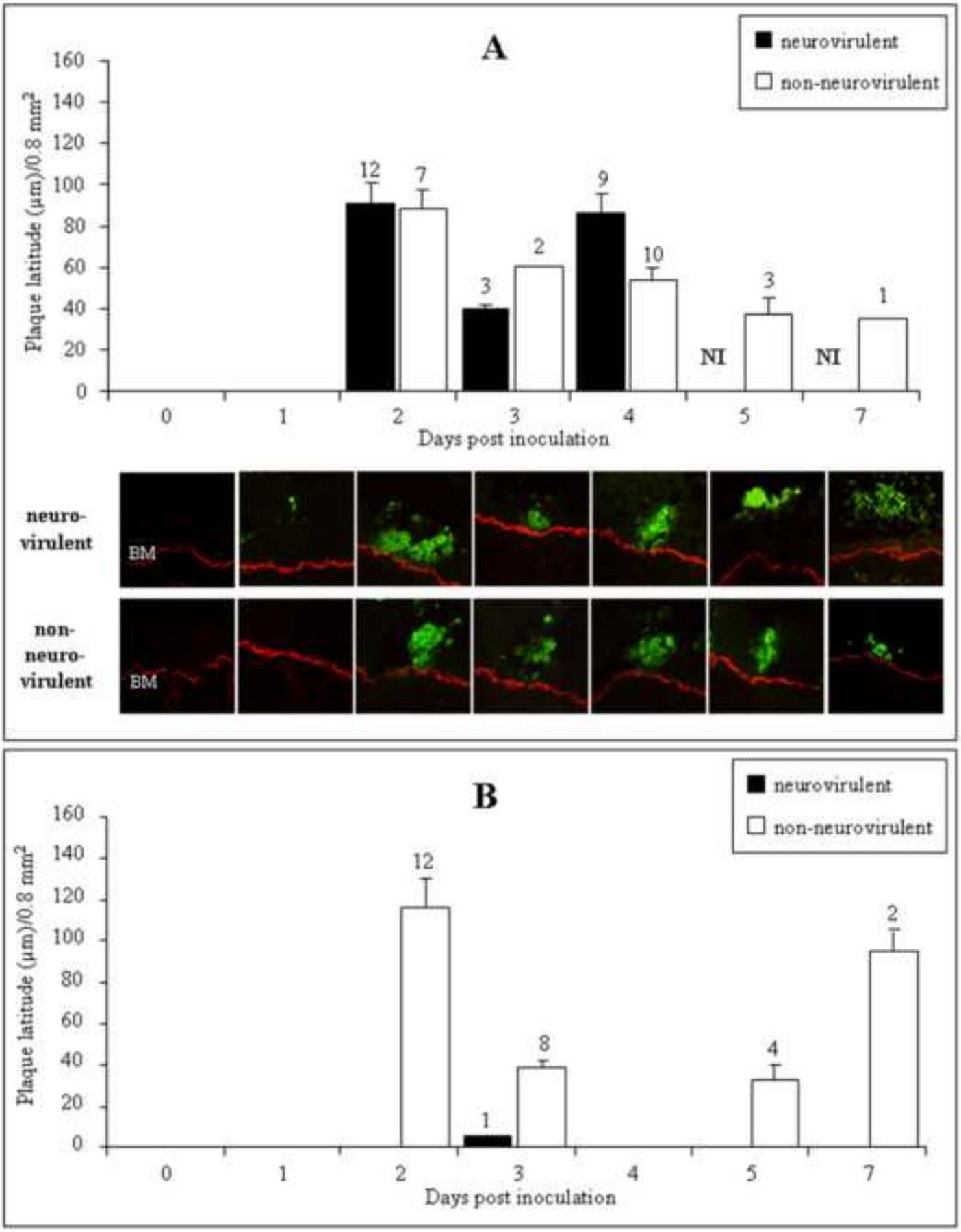

Fig 3 Gryspeerdt *et al.*

Schematic overview of the structure of the nasal septum and different counting regions

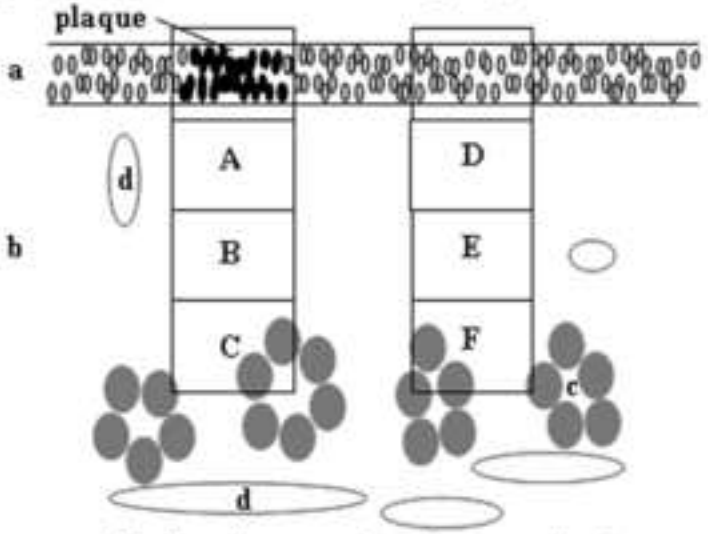

a: epithelium; b: connective tissue; c: glands; d: blood vessel

Strain	Roi	Total number of single infected cells present at … dpi/30 sections						
		0	1	2	3	4	5	7
Neurovirulent	A	-	-	34	17	34	137	82
	B	-	-	52	13	62	8	60
	C	-	-	24	8	40	4	18
	D	0	3	24	34	62	11	9
	E	0	0	24	10	58	11	5
	F	0	0	28	9	22	8	2
Non-neurovirulent	A	-	-	3	0	4	1	0
	B	-	-	4	3	15	0	0
	C	-	-	0	1	0	0	0
	D	0	0	6	0	19	8	0
	E	0	0	0	0	17	6	0
	F	0	0	0	0	25	3	0

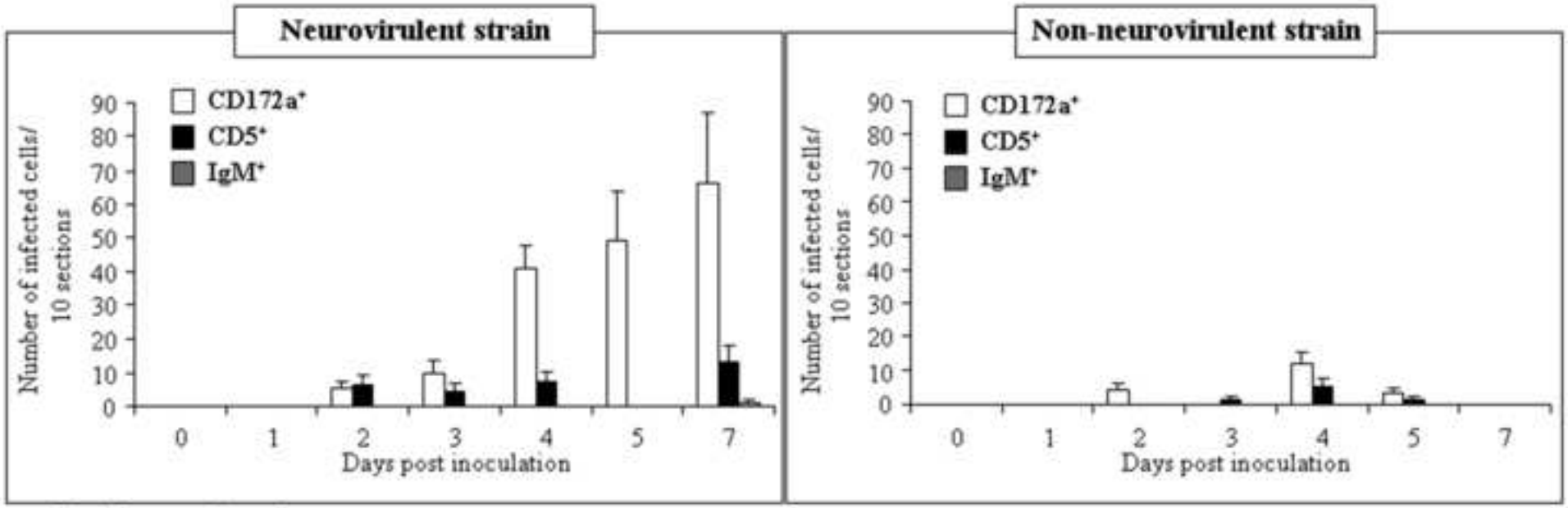

Fig 4 Gryspeerdt *et al.*

Schematic overview of the structure of the nasopharynx and different counting regions

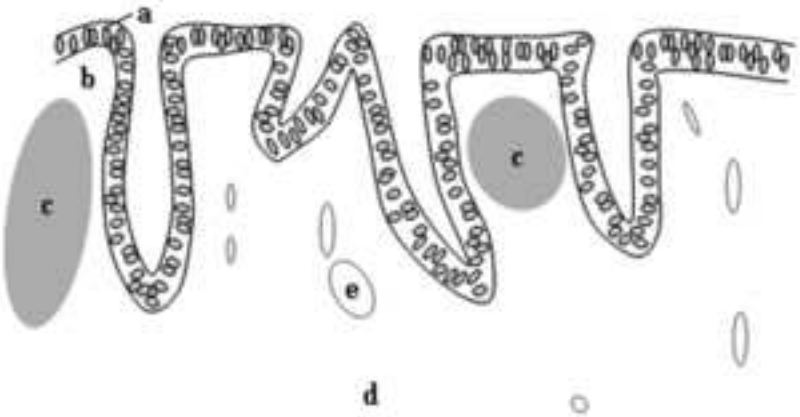

a: epithelium; b: connective tissue; c: lymphocyte aggregate; d: deeper connective tissue; e: blood vessels

Strain	Roi	Total number of single infected cells present at ... dpi/30 sections						
		0	1	2	3	4	5	7
Neurovirulent	a	0	3	3	7	2	0	1
	b	0	22	24	118	22	18	23
	c	0	0	0	0	0	0	0
	d	0	0	0	0	0	0	0
	e	0	0	0	0	0	0	0
Non-neurovirulent	a	0	0	0	0	0	0	0
	b	0	1	320	15	28	18	1
	c	0	0	0	0	99	16	1
	d	0	0	0	0	0	0	0
	e	0	0	0	0	0	1	0

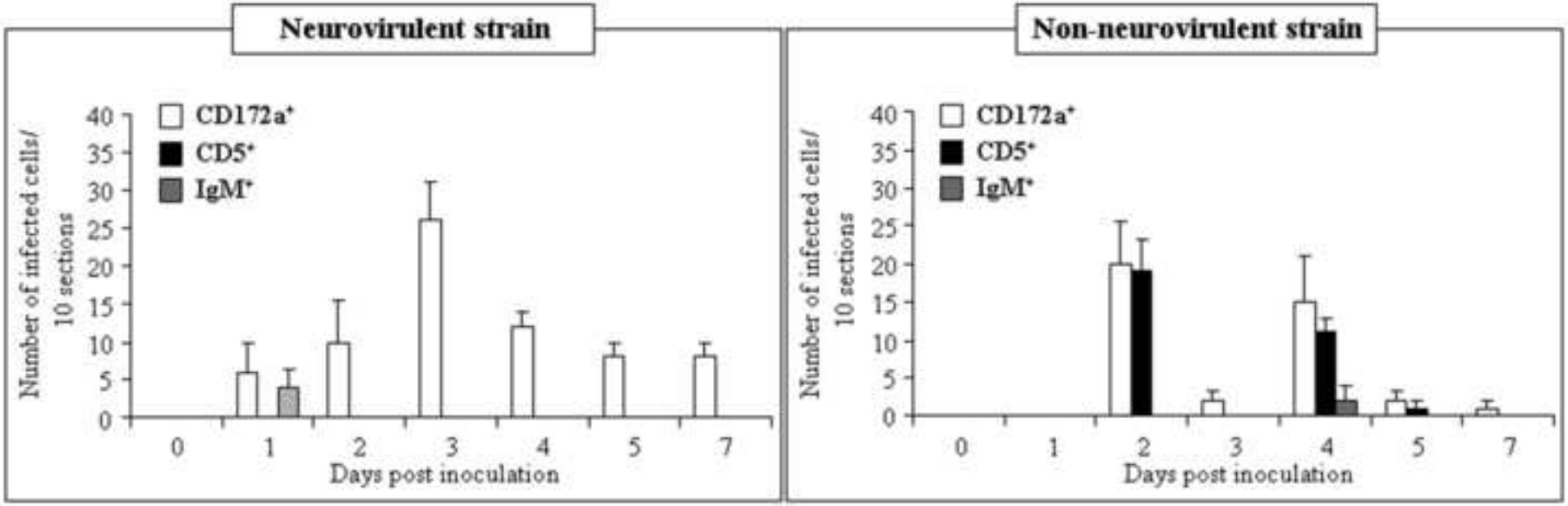

Fig 5 Gryspeerdt *et al.*

Schematic overview of the structure of tubal and nasopharyngeal tonsils and different counting regions

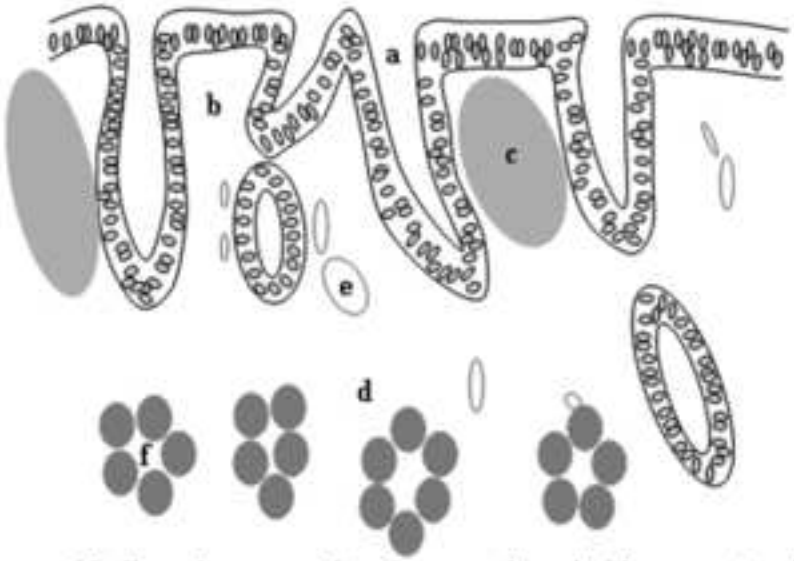

a: epithelium; b: connective tissue; c: lymphoid aggregate; d: deeper connective tissue; e: blood vessel; f: glands

Strain	Roi	Total number of single infected cells present at ... dpi/30 sections						
		0	1	2	3	4	5	7
Neurovirulent	a	0	0	5	77	95	0	14
	b	0	0	6	273	538	1	51
	c	0	0	3	260	241	2	0
	d	0	0	0	86	150	2	7
	e	0	0	0	133	85	0	2
	f	0	0	0	38	117	1	13
Non-neurovirulent	a	0	0	7	23	7	18	5
	b	0	0	39	173	51	50	2
	c	0	0	10	34	31	487	8
	d	0	0	44	78	14	8	2
	e	0	0	0	5	3	0	2
	f	0	0	2	0	2	4	13

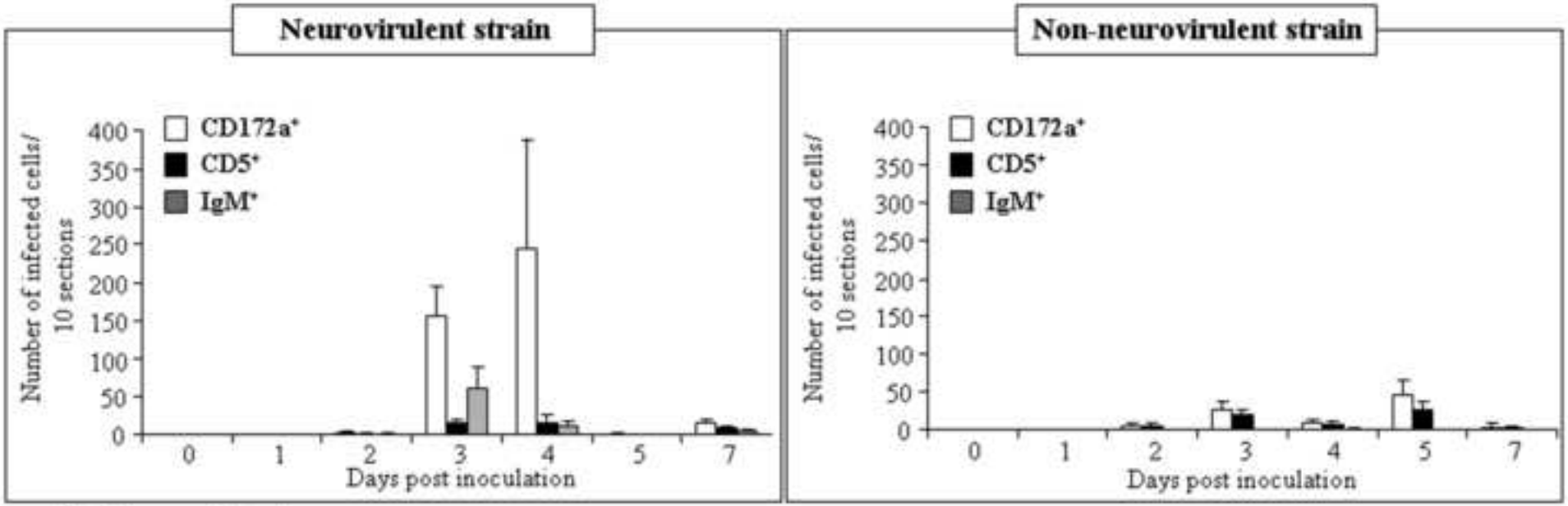

Fig 6 Gryspeerdt *et al.*

Schematic overview of the structure of the mandibular lymph node and different counting regions

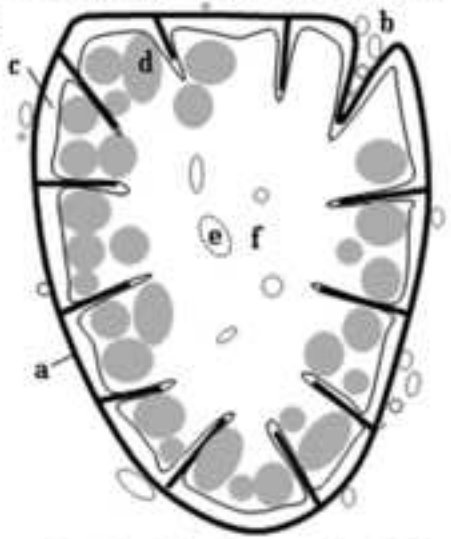

a: capsule and trabecula; b: vessels of the capsule; c: marginal sinus; d: cortical nodule; e: vessels in medulla; f: medulla

Strain	Roi	Total number of single infected cells present at … dpi/30 sections						
		0	1	2	3	4	5	7
Neurovirulent	a	0	0	0	40	10	162	1
	b	0	12	2	16	40	12	0
	c	0	17	6	106	846	170	34
	d	0	2	2	31	36	4	19
	e	0	0	0	3	1	0	0
	f	0	0	9	49	70	14	39
Non-neurovirulent	a	0	0	0	0	4	5	1
	b	0	0	0	0	0	0	0
	c	0	1	2	4	40	39	1
	d	0	0	0	0	5	17	8
	e	0	0	0	0	0	0	0
	f	0	0	0	0	41	82	1

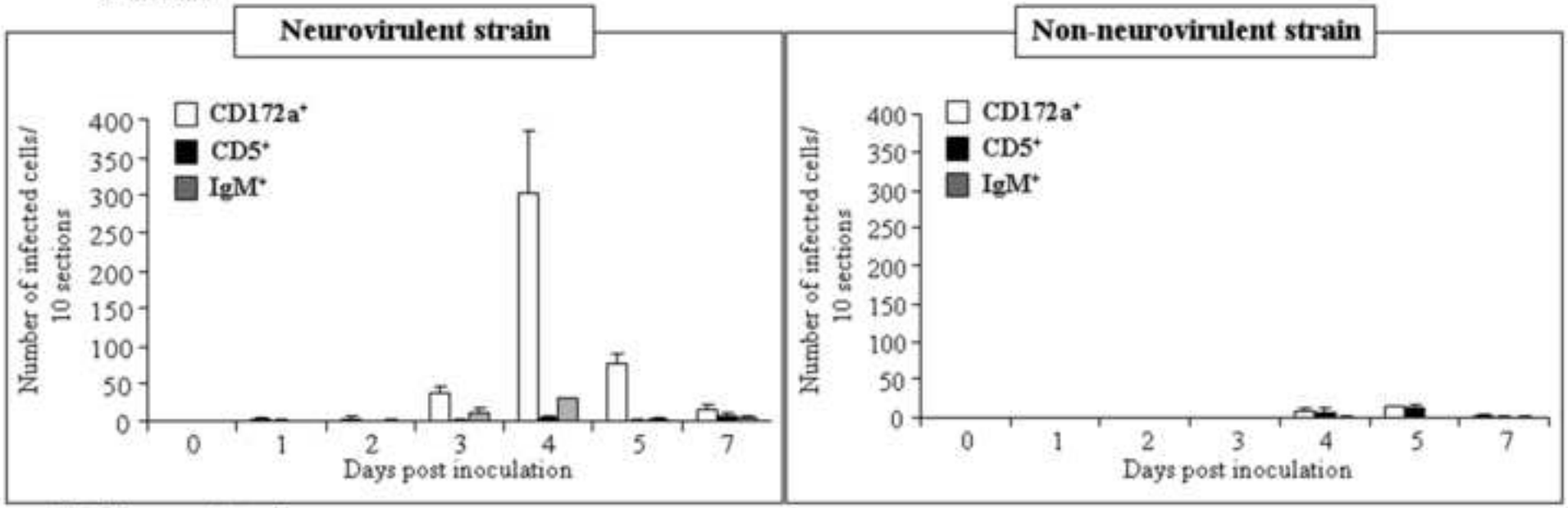

Fig 7 Gryspeerdt *et al.*

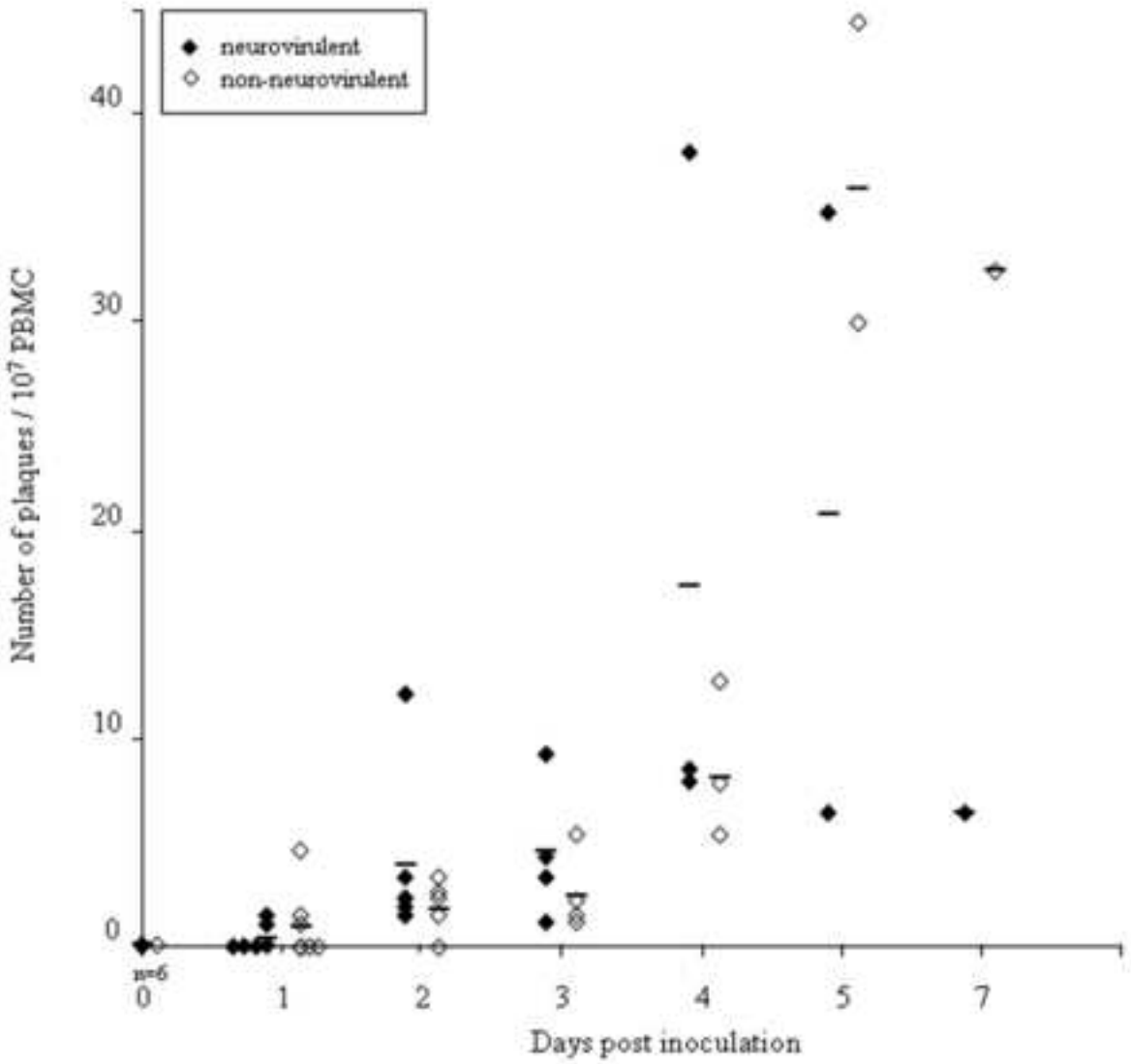

Fig 8 Gryspeerdt *et al.*